The Influence of Al_3Zr Dispersoids on the Recrystallization of Hot-Deformed AA 7010 Alloys

BRUCE MORERE, CLAIRE MAURICE, RAVI SHAHANI, and JULIAN DRIVER

The recrystallization of AA 7010 alloys (Al-6 pct Zn-2.4 pct Mg-1.6 pct Cu-Zr) during solution treatment is investigated as a function of Zr content after deformation under conditions simulating hot rolling. The respective roles of the volume fraction and size of Al_3Zr dispersoids are characterized by additions of 0.05 to 0.12 pct Zr and suitable heat treatments. Plane strain compression (channel-die) tests at temperatures of 320 °C and 440 °C were conducted to strains of 1, and the samples subsequently solution-annealed at 470 °C. Recrystallization during this anneal was characterized by optical and electron microscopy and X-ray diffraction. The fraction recrystallized decreases with increasing Zr content, higher deformation temperature, and finer particle size. An original model based on the concept of the recrystallizable volume fraction is presented to predict the degree of recrystallization in materials characterized by spatially heterogeneous microstructures.

I. INTRODUCTION

THE AA7010 (Al-Zn-Mg-Cu) alloy is widely used for structural components in critical aerospace applications such as wing spars. The essential properties that combine high yield stress and good fracture toughness are obtained by a combination of thermomechanical processing and age hardening. The processing includes hot rolling and cooling to room temperature followed by a solution treatment, quenching, and aging. The aging reactions and their influence on the mechanical properties of these alloys have been widely studied.[1,2,3] However, it is now recognized that the critical fracture toughness properties can be strongly influenced by the amount of recrystallization that occurs during the solution treatment as a consequence of the energy stored during hot rolling. In general, the higher the degree of recrystallization, the lower the fracture toughness, so that manufacturers try to inhibit recrystallization by the addition of Zr, which forms fine Al_3Zr dispersoids.

Clearly, both the hot rolling conditions and the alloy content have to be optimized to obtain suitable microstructures for the required properties. In this article, the specific influences of the size and volume fraction of Al_3Zr dispersoids are analyzed by controlled hot deformation tests on a series of 7010 alloys of varying Zr contents (0.05 to 0.12 pct).

The hot rolling conditions are simulated by instrumented high-temperature plane strain channel-die compression (PSC) tests under conditions of constant temperature and strain rate. This deformation method gives relatively homogeneous deformations and direct flow stress data and enables the sample to be quenched. The microstructures are characterized by quantitative optical and electron metallography, including transmission electron microscopy (TEM) and scanning electron microscopy–electron backscattered diffraction (SEM-EBSD). Particular attention is paid to the size and spatial distribution of the Al_3Zr dispersoids, which tend to be distributed very heterogeneously within the grains. This heterogeneous dispersoid distribution has a pronounced effect on the fraction of material that is capable of recrystallizing for a given set of conditions.

BRUCE MORERE, Research Engineer, and RAVI SHAHANI, R & D Program Leader, are with the Pechiney Centre de Recherche de Voreppe, 38341 Voreppe Cedex, France. CLAIRE MAURICE, CNRS Scientist, and JULIAN DRIVER, Research Director, are with the Microstructures and Processing Department, Ecole des Mines, 42023 Saint Etienne, France.

Manuscript submitted February 22, 2000.

II. EXPERIMENTAL PROCEDURE

Four experimental (10 kg) casts of different Zr contents, denoted A, B, C, and D, were prepared at the Pechiney CRV research center. Their compositions are given in Table I, along with that of a standard 7010 alloy denoted R. Apart from the Zr contents, the other alloying elements have levels close to those of the reference.

The compression samples cut out from the ingots were homogenized 24 hours at 480 °C, using one of two heating rates: slow at 0.3 °C/min and rapid at 11 °C/min. The heating rate is important, since Zr precipitates out as Al_3Zr dispersoids, which then coarsen during the heating stage. Faster heating rates facilitate dissolution of the finer, unstable dispersoids and therefore tend to form coarser dispersoids. After homogenization, the samples were quenched to room temperature.

Plane strain channel-die compression tests were conducted in a modified version of a hot channel-die equipment described by Maurice and Driver.[4] Samples 7 mm in width, 14 mm in height, and 18 mm in length were placed in the preheated dies, after being lubricated by means of a combination of Teflon film and graphite spray. Heating, and time-to-temperature stabilization take approximately 3 minutes. The samples were deformed to a strain of unity (71 pct reduction) at a constant strain rate of 1 s^{-1} and at two temperatures, 320 °C and 440 °C. Immediately after deformation, the samples were quenched in ~2 seconds by opening the mobile die wall and pushing the sample into a water bath. Solution treatments to partial or complete recrystallization were carried out in a salt bath at 470 °C for 6 hours, followed by a quench.

Metallographic sections were taken principally from the longitudinal RD/ND plane. Optical microscopy was used to characterize the Al_3Zr dispersoid distribution (Section III), and the fraction recrystallized by means of an image analysis

Table I. Alloy Compositions in Weight Percent

Alloy	Si	Fe	Cu	Mg	Zn	Zr	Cu + Mg + Zn
7010-A	0.051	0.064	1.59	2.29	6.12	0.053	10.0
7010-B	0.053	0.064	1.55	2.26	5.95	0.082	9.76
7010-C	0.034	0.062	1.61	2.24	6.01	0.105	9.86
7010-D	0.037	0.063	1.54	2.16	5.85	0.120	9.55
7010-R	0.06	0.10	1.65	2.37	6.08	0.11	10.1

technique. The TEM was carried out in a PHILIPS* CM 200 to characterize the Al_3Zr particle sizes and the dislocation substructures.

*PHILIPS is a trademark of Philips Electronic Instruments Corp., Mahwah, NJ.

III. RESULTS AND DISCUSSION

A. *Al_3Zr Dispersoids*

In industrial practice, Al_3Zr precipitates in the Zr-rich zones of the grains during heating of the as-cast ingots to the homogenization temperature. As a consequence of the peritectic solidification reaction, Zr segregates to the dendrite cores, so that subsequent Al_3Zr precipitation occurs principally in the grain centers, and an Al_3Zr dispersoid-free zone can form between the grain boundary region and the center.

To characterize the spatial heterogeneity of the Al_3Zr dispersoids 10 to 50 nm in size within grains 200 to 300 μm in size, a special marker technique was used. Selected hot deformed samples were solutionized for 1 hour at 470 °C, then air-cooled to allow precipitation of micrometer-sized η ($MgZn_2$) particles on the Al_3Zr dispersoids. An orthophosphoric acid etch then reveals the η precipitates and, therefore, the locations of the Al_3Zr dispersoids. Figure 1 gives an example of the low Zr 7010-A alloy after both slow and rapid heating rates. A very heterogenous distribution of precipitates is clearly seen as dark bands, particularly in the recrystallized grains. Recrystallization renders the Al_3Zr dispersoids incoherent, and so favors subsequent η precipitate nucleation on the dispersoids.

The mean size of the Al_3Zr dispersoids was determined by TEM on longitudinal sections of samples, which were hot compressed, to reduce the distances between the bands of dispersoids, and annealed 10 minutes at 470 °C to dissolve the η precipitates. Figure 2 shows examples of dispersoids in the samples after (1) slow and (2) rapid heating. The average Al_3Zr sizes of 15 through 20 nm (slow) and 30 to 35 nm (rapid heating) confirm the major role of the heating rate. Note also that, since the dispersoid volume fractions f_v are constant, the density of the Al_3Zr dispersoids is much greater in the slowly heated material. Equilibrium volume fractions were calculated for the homogenization temperature using standard thermodynamic methods; they indicate 0.042 pct Zr in solid solution and average Al_3Zr dispersoid volume fractions $\bar{f}_v$ of 0.016, 0.055, 0.086, 0.106, and 0.097 pct, respectively, for alloys 7010 A through D and the 7010-R. These average equilibrium values are only indications, since the local volume fractions can vary enormously.

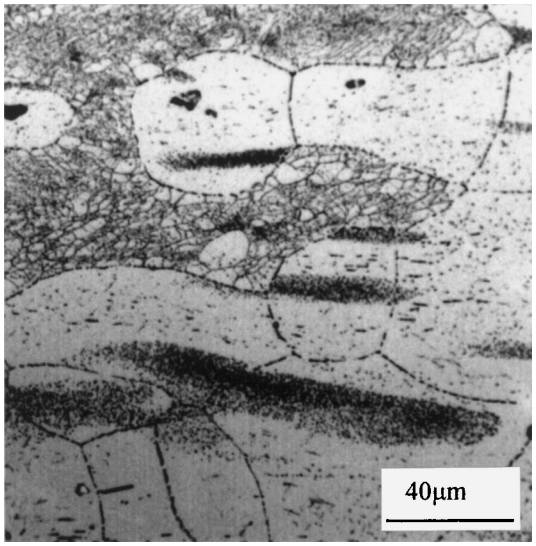

(*a*)

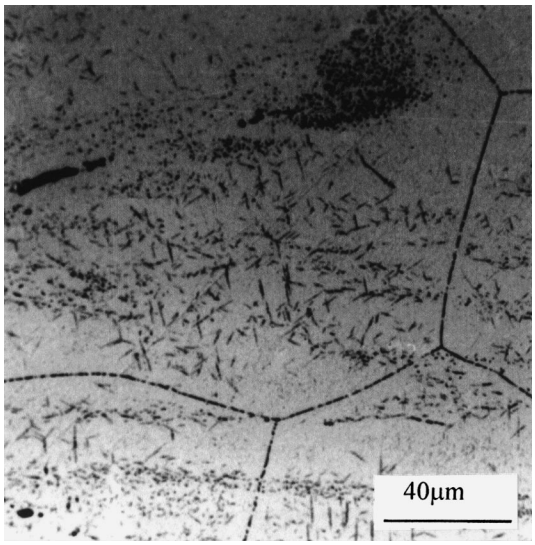

(*b*)

Fig. 1—Spatial distributions of Al_3Zr dispersoids in the grains of the low Zr 7010-A alloy as characterized by optical microscopy of marked dispersoids (text) after (*a*) slow heating and (*b*) rapid heating.

B. *Hot Deformation*

Figure 3 illustrates the stress-strain curves of a typical 7010-Zr alloy and the 7010-R standard at the temperatures of 320 °C and 440 °C. The $\sigma(\varepsilon)$ plots reveal rapid stress saturation at a strain of about 0.1, with some small stress variations thereafter. At 320 °C, the flow stress tends to exhibit slight softening due to some deformation-induced heating; at 440 °C, on the other hand, the applied stress increases somewhat at high strains, probably as a result of some friction effects.

The flow curves are given for the two heating rates of the 7010-Zr alloy, but it is obvious that the prior heating rate has no significant effect on the hot deformation behavior. In fact, the Zr contents investigated here have no apparent effect on the stress-strain curves, which are essentially controlled by the solute content and the temperature and strain rates, as described in Reference 5. The standard rheological

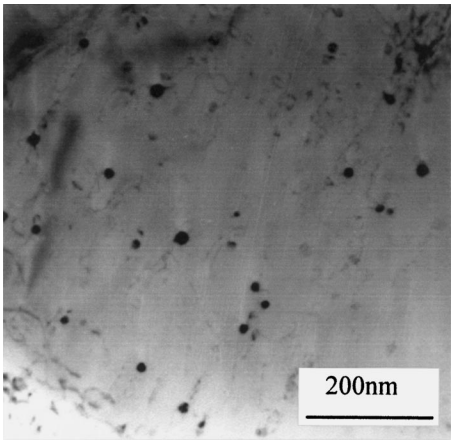

(*a*)

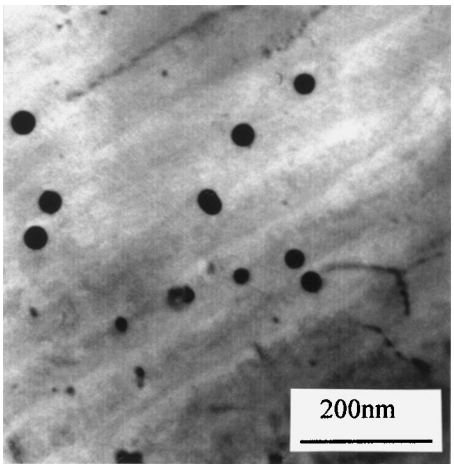

(*b*)

Fig. 2—Al_3Zr dispersoids characterized by TEM after (*a*) slow heating and (*b*) rapid heating.

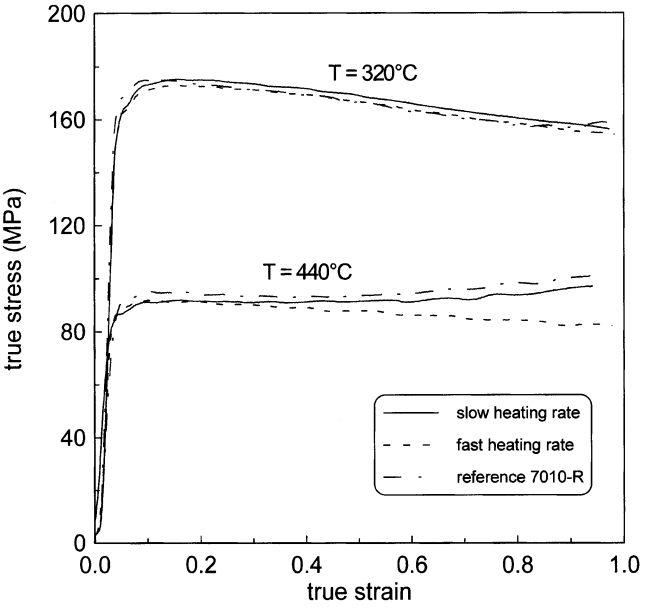

Fig. 3—PSC channel-die stress-strain curves of 7010-R and 7010-C alloys at two temperatures (320 °C and 440 °C); the model alloy is tested after both heating rate conditions.

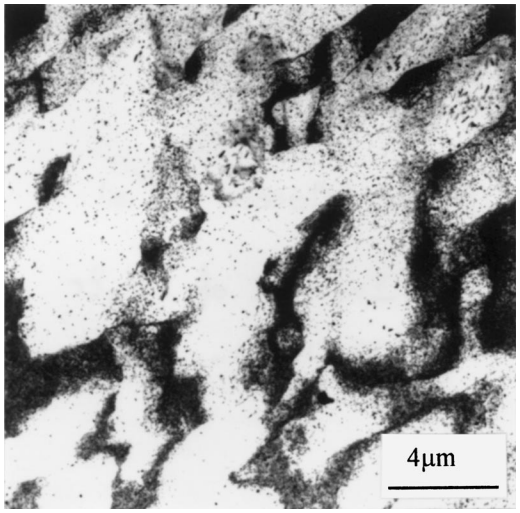

(*a*)

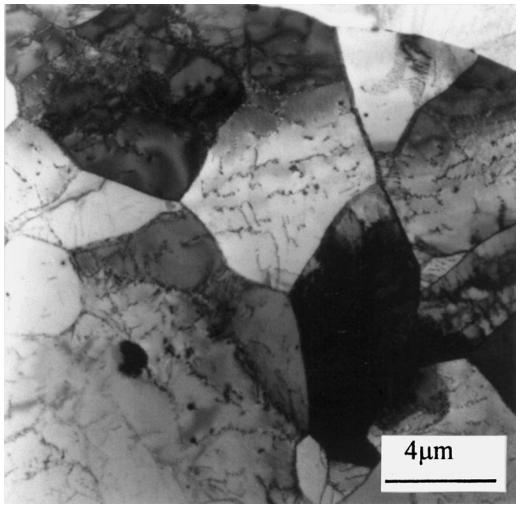

(*b*)

Fig. 4—Typical deformation substructures in 7010-Zr alloy deformed at 1 s^{-1} to a strain of 1: (*a*) 320 °C and (*b*) 440 °C.

parameters $m = \left.\frac{\partial \ln \sigma}{\partial \ln \dot{\varepsilon}}\right|_T$ and the activation energy for deformation $Q = \left.\frac{R \cdot \partial \ln \sigma}{m \cdot \partial (1/T)}\right|_{\dot{\varepsilon}}$ were analyzed for the 7010-R sample.[6] The strain rate sensitivity coefficient m varies between 0.09 and 0.17 for temperatures of 320 °C and 440 °C. The activation energy Q is evaluated at 142 kJ/mol at $\dot{\varepsilon} = 1\ s^{-1}$, reasonably close to the widely used value of 155 kJ/mol for hot deformation of aluminum alloys.

The hot deformation microstructures of the reference alloy, as determined by TEM and SEM-EBSD, are described elsewhere.[6] The influence of the deformation temperature on the subgrain microstructure is shown in Figure 4: at 320 °C, elongated subgrains of size 1 through 3 μm are formed together with a high density of dislocations (and η precipitates), and at 440 °C, larger equiaxed subgrains, 2 to 4 μm in size, relatively free of dislocations, are developed. The average subgrain misorientations in both cases are between 1 and 2 deg. (Note that these are the substructure features observed by quenching immediately after hot deformation).

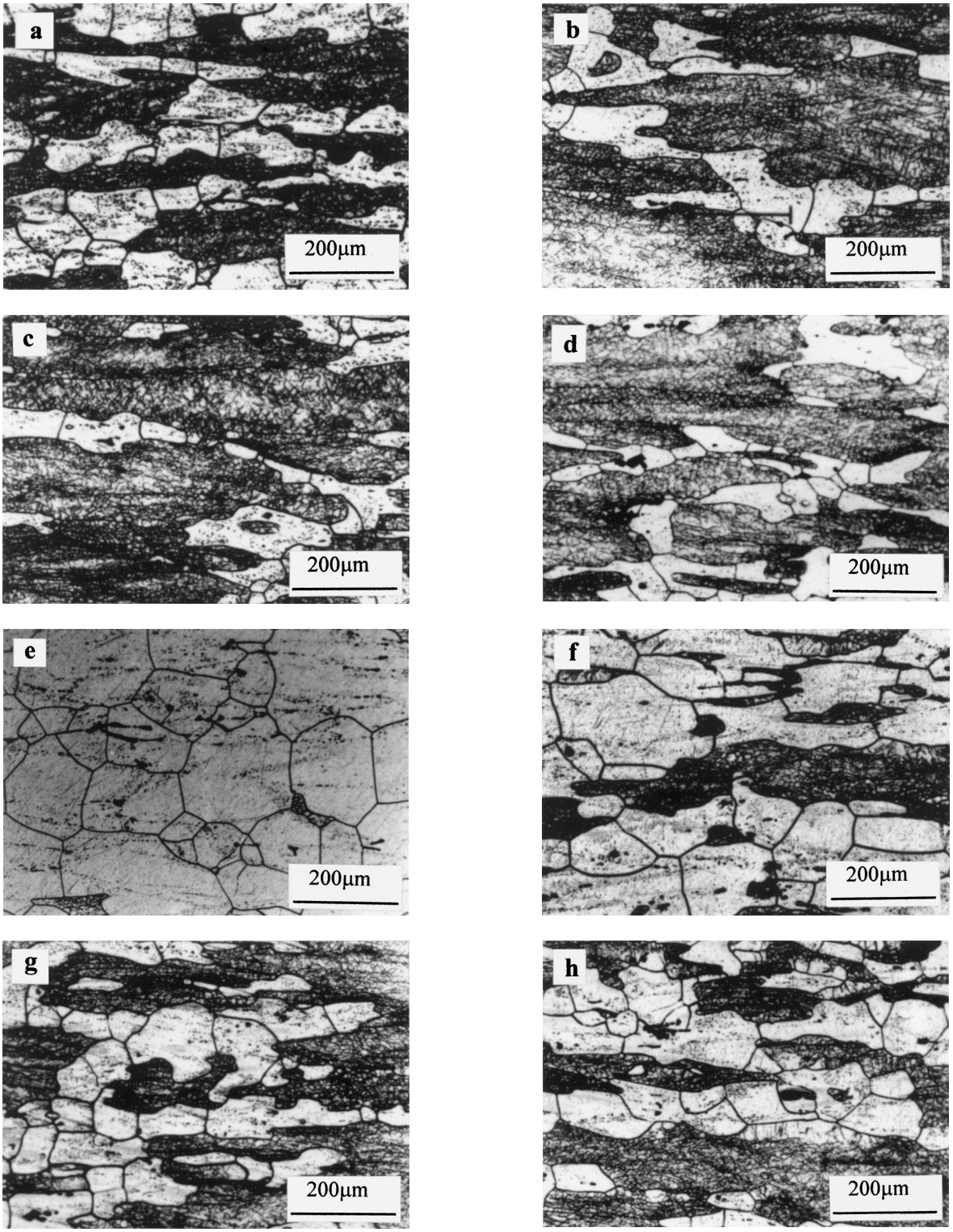

Fig. 5—The influence of Al_3Zr dispersoids on recrystallization. Optical micrographs (orthophosphoric etch) on longitudinal (ND/RD) section of the four model alloys deformed at 440 °C 1 s^{-1} and solutionized 6 h at 470 °C. Recrystallized grains are light while the non-recrystallized (dark) areas contain subgrains decorated by precipitates. (*a*) through (*d*) represent alloys A through D in the slowly heated state and (*e*) through (*h*) the same alloys after rapid homogenization heating.

C. *Recrystallization Behavior*

The optical micrographs of Figure 5 reveal the typical partially recrystallized microstructures developed in the alloys after the solution treatment for 6 hours at 470 °C, following the hot PSC deformation at 440 °C. There is clearly a strong influence of both the Zr content and the heating rate prior to homogenization. After a high heating rate to form the larger Al_3Zr dispersoids, the recrystallized volume fraction X can vary from 95 pct (0.05 pct Zr) to 40 pct (0.1

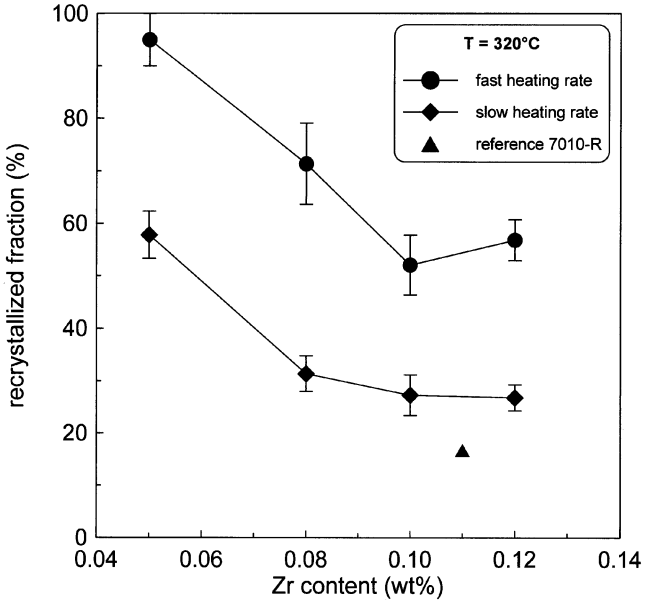

(*a*)

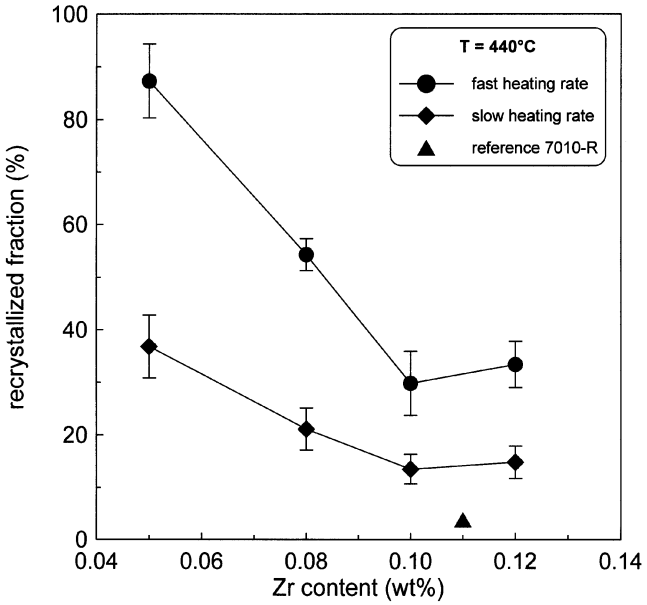

(*b*)

Fig. 6—The recrystallized volume fractions as a function of Zr content for both prior heating rates: (*a*) deformed at 320 °C and (*b*) deformed at 440 °C.

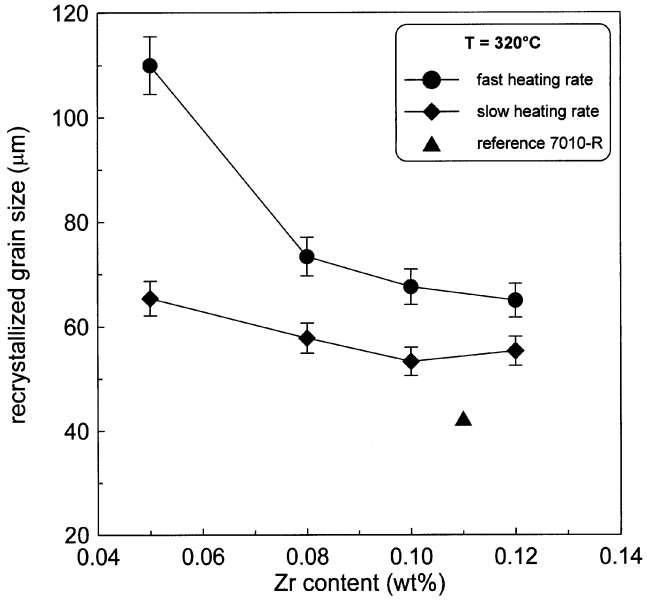

(*a*)

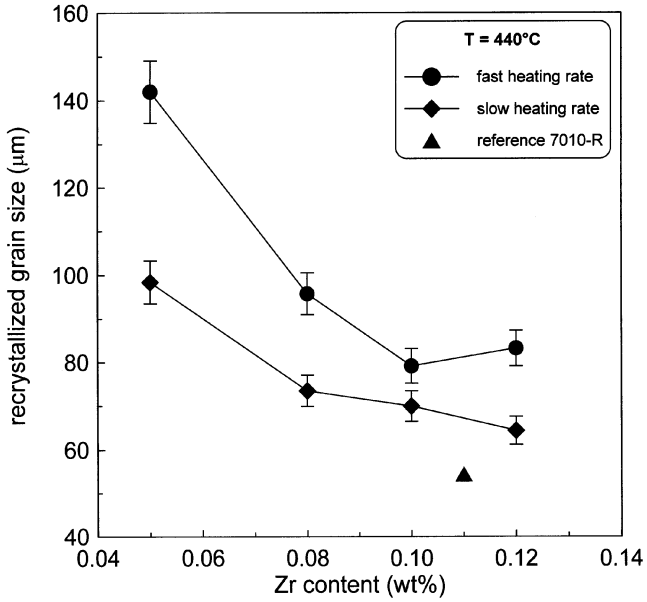

(*b*)

Fig. 7—The average recrystallized grain size as a function of Zr content for both prior heating rates: (*a*) deformed at 320 °C and (*b*) deformed at 440 °C.

pct Zr). The slower heating rate gives significantly lower amounts of recrystallization, varying between about 40 and 20 pct for the Zr-rich alloys.

Similar trends are observed after deformation at 320 °C, but the recrystallized fractions are generally higher, as a consequence of the higher stored energy of deformation.

Figure 6 plots out the X(Zr) volume fractions for the deformation temperatures of (a) 320 °C and (b) 440 °C. The average recrystallized grain size is also given in Figure 7 as a function of the same parameters: finer grain sizes are obtained on the slowly heated samples of high Zr contents deformed at the lower temperature.

It is apparent from the optical micrographs that recrystallization is quite heterogeneous at the grain scale and occurs principally along the grain boundary regions of the as-deformed grains. The grain centers recrystallize only in the very low Zr alloys, if they do recrystallize at all. The recrystallized grains often contain large, constituent, intermetallic particles on which particle stimulated nucleation (PSN) is considered to take place. The PSN generally results in recrystallized grains of fairly random orientation: this is born out by the texture analysis. The typical hot rolling textures developed by the PSC tests are strongly attenuated by this partial recrystallization.[7]

D. *Analysis of the Recrystallizable Volume Fractions X^R*

1. *Principles*

The present observations of the recrystallization behavior of these microstructurally heterogeneous 7010 alloys indicate that parts of the grains can recrystallize easily: the grain boundary areas along which PSN occurs on the large constituent particles and where the Zener drag effect due to the fine dispersoids is weak. Other areas, particularly the grain centers in the Zr-rich alloys, simply do not recrystallize. The size and local volume fractions of the Al_3Zr dispersoids, therefore, have a pronounced influence on the resulting grain structure. It is proposed that the results can be interpreted in terms of the concept of the recrystallizable volume fraction X^R, the volume fraction in which the driving force for recrystallization is greater than the boundary pinning forces that inhibit recrystallization. This idea is applied here to the case of 7010 alloys, for which the driving force is derived from the dislocation density of the subgrains, and the pinning force is simply due to Zener drag. (The minor effects of boundary curvature on growth of recrystallized grains are neglected, and the solute drag effects are assumed constant for the set of alloys examined. Moreover, since the recrystallization measurements have been made after a relatively long period at high temperature, the system is considered to be near equilibrium, so that kinetic aspects are also ignored.)

The driving force for recrystallization of a hot deformed aluminum alloy is essentially due to the subgrain boundary energies γ_{sg}, their size δ_{sg}, and the misorientation θ_{sg}.[8] For equiaxed subgrains, the driving pressure is

$$P_D = \frac{3\gamma_{sg}}{\delta_{sg}} \qquad [1]$$

where γ_{sg} is given in terms of the subboundary misorientation by the Read–Shockley relation:

$$\gamma_{sg} = \gamma_0 \frac{\theta_{sg}}{\theta_0}\left[1 - \ln\frac{\theta_{sg}}{\theta_0}\right] \qquad [2]$$

where γ_0 is the energy of a high angle boundary at θ_0 (often taken as 15 deg). The pinning force due to Zener drag is usually taken as

$$P_Z = \frac{3 \cdot f_v \cdot \gamma}{d} \qquad [3]$$

where γ is the specific energy of the moving boundary ($\approx \gamma_0$) and d the particle diameter. If, as in the present case, the dispersoid particles are coherent, the pinning force P_Z is multiplied by a factor of 2 to allow for the loss of coherency as the boundary migrates past the particle.[9]

2. *Estimation of the local volume fraction of dispersoids, f_v*

As pointed out above, the local volume fraction f_v of the dispersoids varies strongly within the grains, as a result of peritectic solidification. This implies that the Zener drag pinning force P_Z also depends on the position within the grain. In order to calculate the recrystallizable volume fraction X^R, it is necessary to evaluate the variations of f_v within a grain. This is done by using the thermodynamic *Prophase* software developed at Pechiney CRV.[10] The calculation is performed in two steps as follows:

(1) Given the average Zr content of the alloy, the local concentration of Zr in solid solution within a grain during solidification can be calculated.[10] During the peritectic solidification reaction within individual grains of the Al-Zr alloys, the local Zr concentration gradually decreases from the center to the boundary of the grain. At any instant, the value of the solidified volume fraction F_s defines a position within the grain: in the initial stages of solidification, F_s is close to 0 (center of the grain), and at the end of solidification, F_s is close to 1 (grain boundary). The variations of Zr concentration with F_s, therefore, represent the distribution of Zr concentration within the grain from the center to the boundary. It should be mentioned that no particular assumption is made concerning the geometry of the grain: the use of the parameter F_s to define the position within the grain enables any grain geometry to be treated.

(2) During the homogenization treatment at 480 °C that follows casting of the billets, Zr can precipitate out as Al_3Zr dispersoids. Given the local concentration in Zr, the local volume fraction of dispersoids is calculated as the equilibrium volume fraction at the homogenization temperature. At positions within the grain where the Zr concentration exceeds the solid solubility, Al_3Zr dispersoids precipitate out. Conversely, if the local Zr concentration is less than the solid solubility, dispersoids should not form. Because of the initial Zr concentration profile within the grain, the local volume fraction of dispersoids gradually decreases from the center of the grain and reaches 0 at a position where the initial Zr concentration equals the solid solubility at the homogenization temperature. A position within the grain is defined by the parameter ξ (numerically identical to F_s), which represents the relative volume of the grain from the center ($\xi = 0$) to the boundary ($\xi = 1$).

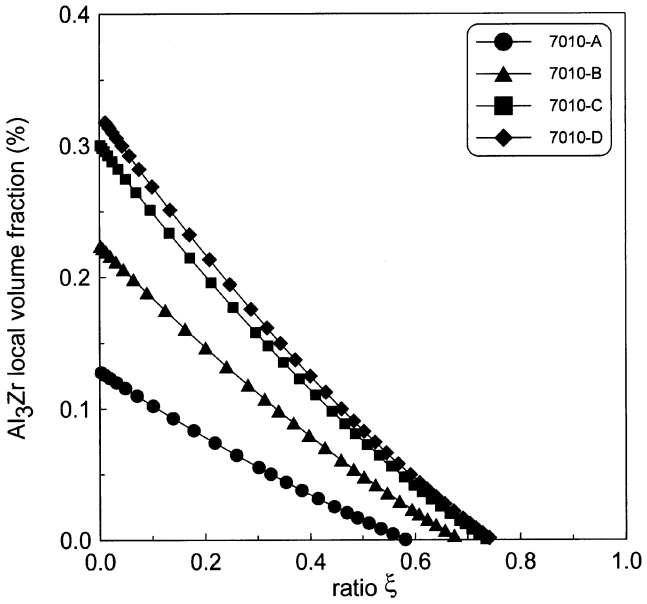

Fig. 8—Calculated Al_3Zr dispersoid volume fractions across a grain from the center ($\xi = 0$) to the boundary ($\xi = 1$) for the four model alloys (text).

The results are given graphically in Figure 8 in the form of $f_v(\xi)$ plots for the four different experimental alloys. The position at which $f_v(\xi)$ reaches 0 is denoted ξ_0. The parameter $(1 - \xi_0)$ characterizes the extent of the dispersoid-free zone

Table II. Calculated Average and Maximum Dispersoid Volume Fractions and the Relative Threshold Distances ξ_0 at Which the Zr Solubility Limit Is Attained

Alloy Zr Content (Wt Pct)	$\bar{f}_v$ (Pct)	f_{max} (Pct)	ξ_0
0.053	0.016	0.13	0.58
0.082	0.055	0.22	0.68
0.105	0.086	0.30	0.73
0.120	0.106	0.32	0.74

close to the grain boundary: if $\xi_0 = 0.8$, then 20 pct of the grain volume is free of dispersoids. The value of ξ_0 depends on the alloy. Table II indicates the ξ_0 values and the maximum dispersoid volume fractions f_{max} expected for the different alloys.

It can be seen from Figure 8 that the spatial variation of f_v across a grain can be approximated by a linear function of the form

$$f_v = f_{max}\left[1 - \frac{\xi}{\xi_0}\right] \quad [4]$$

3. *The recrystallizable volume fractions*

Substituting for f_v (from Eq. [4] into Eq. [3]) gives the variation of P_Z across a grain. Let us call ξ_R the relative volume fraction of the grain for which the Zener pinning force is larger than the driving pressure, *i.e.*, $P_Z \geq P_D$; the recrystallizable volume fraction X^R is then linked to ξ_R by the relation

$$X^R = 1 - \xi_R \quad [5]$$

Equating P_Z to P_D at the critical position ξ_R gives the recrystallizable volume fraction X^R as

$$X^R = 1 - \xi_0\left[1 - \frac{P_D \cdot d}{6 \cdot f_{max} \cdot \gamma}\right] \quad [6]$$

where ξ_0 and f_{max} have been calculated and are given in Table II. The other parameter required to evaluate X^R is the driving force P_D, given by Eqs. [1] and [2] as a function of the sub-boundary energies and subgrain sizes. The values used here are $\gamma_0 = 0.324$ J m^{-2}, $\theta_0 = 15$ deg and $\theta_{sg} = 1.5$ deg. The subgrain sizes δ_{sg} are taken as 6 μm and 10 μm for the deformation temperatures of 320 °C and 440 °C, respectively. These values are significantly greater than the subgrain sizes in the as-deformed state, but correspond to the sizes measured after a few hours at 470 °C, when substantial recovery has occurred. Note that P_D is assumed constant over the grain volume. The Zener pressure $P_z(\xi)$ is determined from Eq. [3] for different dispersoid sizes (d = 5, 15, and 35 nm), using the $f_v(\xi)$ values evaluated for the different Zr contents, as outlined previously.

The results are given in Figure 9 as plots of $X = f$(pct Zr) for three dispersoid particle diameters, and compared with the experimental volume fractions of recrystallized material for the two deformation temperatures. The sets of experimental volume fractions are given for the two heating rates corresponding to Al_3Zr dispersoid sizes of 15 and 35 nm.

The model reproduces qualitatively the experimental results quite well; the well-known influences of the dispersoid size and volume fraction, respectively, are predicted

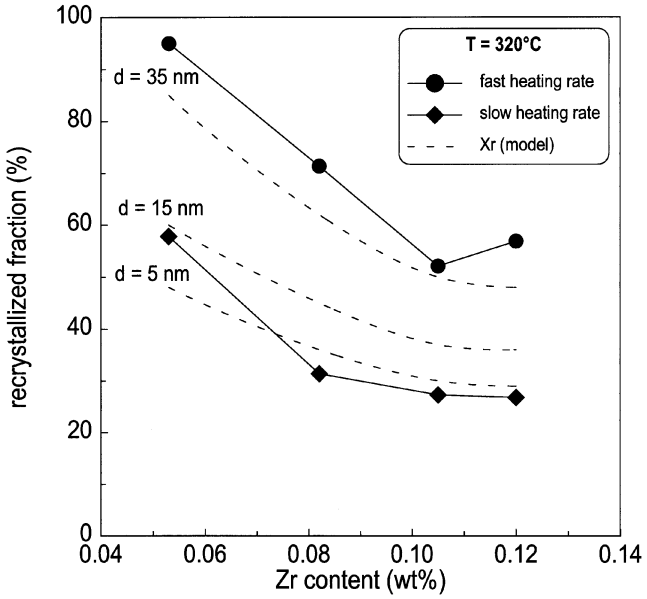

(*a*)

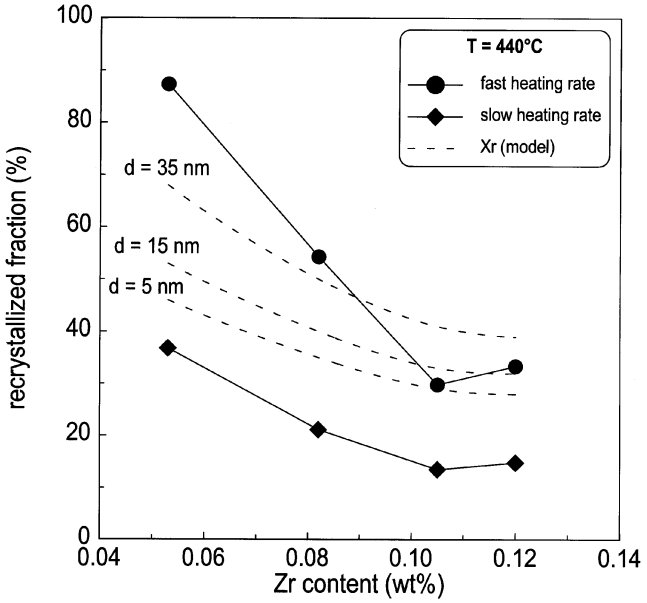

(*b*)

Fig. 9.—The predicted and experimental recrystallized volume fractions as a function of alloy Zr content for different dispersoid sizes: (*a*) deformed at 320 °C and (*b*) deformed at 440 °C.

with reasonable accuracy. Furthermore, the model predicts the following features.

(1) The influence of the Zr content decreases at higher Zr levels. Above a certain Zr content of about 0.1 pct, the dispersoid density within the grain center attains a value that completely inhibits recrystallization. The recrystallizable volume fraction, therefore, becomes less solute dependent and tends to the limiting value of $(1 - \xi_0)$.
(2) The size of the dispersoids is particularly important at low Zr contents. This effect is seen most clearly in the experimental results on the alloy deformed at 440 °C. In fact, at high Zr contents, the dispersoid density is such that recrystallization is very difficult regardless of

the size. At lower Zr levels, the reduced dispersoid density enables their size to play a major role.

From a strictly quantitative point of view, the model gives relatively good predictions for the larger (35 nm) dispersoids obtained by rapid heating. However, the slowly heated state with finer dispersoids tends to recrystallize significantly less than predicted by the model for the 15 nm dispersoids (*i.e.*, the experimental value measured by TEM) and appears closer to that expected for dispersoids of 5 nm diameter. This may be related to a number of factors that tend to reduce recrystallization and that have been neglected in the present analysis. For example, it is assumed here that equilibrium quantities of recrystallization are attained in all cases, but this may not be exact for slowly recrystallizing systems containing fine dispersoids. In fact, in these complex industrial alloys, many of the model parameters (*e.g.*, P_z and P_D) usually vary somewhat with time instead of remaining constant, as assumed in the present simplified analysis. The current model should be considered as a semiquantitative guide to understanding the influence of the microstructural parameters.

IV. CONCLUSIONS

1. The recrystallization of model AA 7010 alloys (Al-6 pct Zn-2.4 pct Mg-1.6 pct Cu-Zr) during solution treatment is investigated as a function of Al_3Zr dispersoid size and volume fraction after deformation under conditions simulating hot rolling. The Al_3Zr volume fraction and size were varied by appropriate additions of Zr (0.05 to 0.12 wt pct) and controlled heating rates up to the homogenization temperature.
2. The PSC (channel-die) tests at temperatures of 320 °C and 440 °C were conducted to strains of 1 and the subsequent recrystallization at 470 °C, followed by optical and electron microscopy and X-ray diffraction.
3. The fraction recrystallized decreases with increasing Zr content, higher deformation temperature, and finer particle size.
4. An original model based on the concept of the recrystallizable volume fraction is presented to predict the degree of recrystallization in materials characterized by spatially heterogeneous microstructures. The recrystallizable volume fraction is defined as the volume fraction in which the driving force for recrystallization is greater than the boundary pinning forces that inhibit recrystallization.

ACKNOWLEDGMENTS

This work has been carried out in partial fulfilment of a doctoral thesis (BM) cofinanced by the CNRS and Pechiney. The authors also thank the referee for some pertinent comments.

REFERENCES

1. J.A. Wagner and R.N. Shenoy: *Metall. Mater. Trans. A*, 1991, vol. 22A, pp. 2809-18.
2. R.C. Dorward and D.J. Beernsten: *Metall. Mater. Trans. A*, 1995, vol. 26A, pp. 2481-84.
3. N.U. Deshpande, A.M. Gokhale, D.K. Denzer, and J. Liu: *Metall. Mater. Trans. A*, 1998, vol. 29A, pp. 1191-1201.
4. C. Maurice and J.H. Driver: *Acta Metall. Mater.*, 1993, vol. 41, pp. 1653-64.
5. T. Sheppard and A. Jackson: *Mater. Sci Technol.*, 1997, vol. 13, pp. 203-09.
6. B. Morere: Ph.D. Thesis, Ecole des Mines de Saint Etienne-INPG, Saint Etienne, France, 1999.
7. B. Morere, C. Maurice, J.H. Driver, and R. Shahani: *Proc. ICAA5*, J.H. Driver, B. Dubost, F. Durand, R. Fougeres, P. Guyot, P. Sainfort, and M. Suery, eds., Trans Tech Publications, Aedermannsdorf, Switzerland, 1996, pp. 517-22.
8. F.J. Humphreys and M. Hatherly: *Recrystallization and Related Annealing Phenomena*, Pergamon Press, Elmsford, NY, 1996.
9. E. Nes, N. Ryum, and O. Hunderi: *Acta Metall.*, 1985, vol. 33, pp. 11-22.
10. C. Sigli, L. Maenner, C. Sztur, and R. Shahani: *Proc. ICAA6*, 1997, vol. 1, pp. 87-98.